§7. Transport of Ion/electron Energy in High T_e Plasmas in the Large Helical Device

Takahashi, H., Nagaoka, K., Nakano, H., Yokoyama, M., Ida, K., Yoshinuma, M., Seki, R., Suzuki, C., Ido, T., Shimizu, A., Osakabe, M., High-T Group, Murakami, S. (Kyoto Univ.)

Confinement improvement is necessary for realization of high-temperature plasmas and is one of the most important issues in toroidal devices. Since the first observation of H mode, various kinds of improved confinement modes have been observed in tokamaks and helical/stellarator devices. An internal-transport barrier (ITB) is characterized by a steep gradient formation in temperature profiles and a decrease in heat diffusivity in the plasma core region.

In the Large Helical Device (LHD), an electron-internal-transport barrier (e-ITB) related to the production of high-T_e plasmas has been realized using strongly center-focused ECRH. However confinement characteristics of e-ITB plasmas have been investigated with regard to an electron, the ion energy transport has not been unclear due to the difficulty of the ion temperature measurement. A charge exchange recombination spectroscopy (CXRS) has been used for a measurement of an ion temperature T_i and a radial electric field E_r in the LHD. However, T_i profile in a high-T_e discharge, which is sustained using ECRH alone, has not been able to be measured using the CXRS system because the neutral gas carried into the LHD by diagnostic neutral beam is too large to maintain the plasma, leading to the radiation collapse. Since 2010, a second 40-keV-perpendicular NBI has been operational in the LHD. This NBI can be used not only for plasma heating but as a diagnostic beam for a CXRS measurement. The NBI has an advantage of less carrying neutral gas into the LHD compared with the existing one. Another CXRS system has also been constructed for T_i measurement using the second perpendicular NBI. The new T_i-measurement system enabled us to investigate the ion transport characteristics of e-ITB plasmas quantitatively.

Figure 1 shows the time evolution of (a) the line-averaged electron density n_{e_fir} and (b) the central electron temperature T_{e0} in a typical high-T_e plasma. In the discharge, the second-perpendicular NBI of 2.8 MW was superposed from 3.7 s to 3.98 s on the plasma sustained using ECRH. The waveforms of ECRH and NBI power are also illustrated in fig.1 (a). One line of EC beam stopped the injection due to an arching at 3.76 s and then the total injection power of ECRH decreased from 4.4 MW to 3.2 MW. The plasma maintained the e-ITB with T_{e0} over 7 keV during the NBI injection and sustained without a radiation collapse even though n_{e_fir} increased gradually due to the decrease of ECRH power and/or to the injection of NBI.

Figure 2 shows the radial profiles of (a) T_i, T_e and the electron density n_e, (b) the plasma space potential V_s and E_r and (c) the heat diffusivity for electron χ_e and ion χ_i in the high-T_e plasma in fig.1. The plasma space potential was measured using a heavy ion beam probe (HIBP). The radial electric field was calculated using a neoclassical transport code GSRAKE. The plasma space potential evaluated as the radial integration of the calculated E_r is illustrated using a solid line in fig .2 (b). The heat diffusivities χ_e and χ_i in fig.2 (c) was normalized by $T_e^{3/2}$ and $T_i^{3/2}$, respectively, to cancel the Gyro-Bohm dependence. An ion temperature profile of a high-T_e plasma was successfully obtained in the first time by means of the CXRS with the second-perpendicular NBI. The neoclassical calculation showed the positive E_r in the plasma whole region and well agreed with the experimental result in the measurable region of HIBP ($0.1 < r_{eff}/a_{99} < 0.65$). The electron-heat diffusivity significantly reduced inside the e-ITB in $r_{eff}/a_{99} < 0.35$. On the other hands, the improvement of the ion thermal confinement related to the transport barrier was not observed.

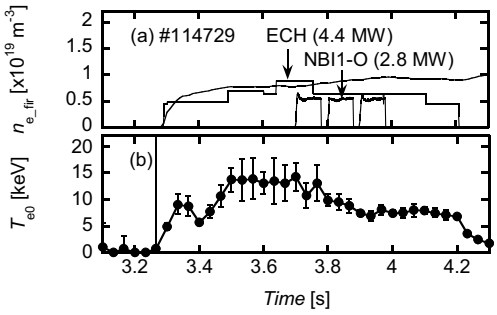

Figure 1. The time evolution of (a) n_{e_fir} and (b) T_{e0} in a typical high-T_e plasma.

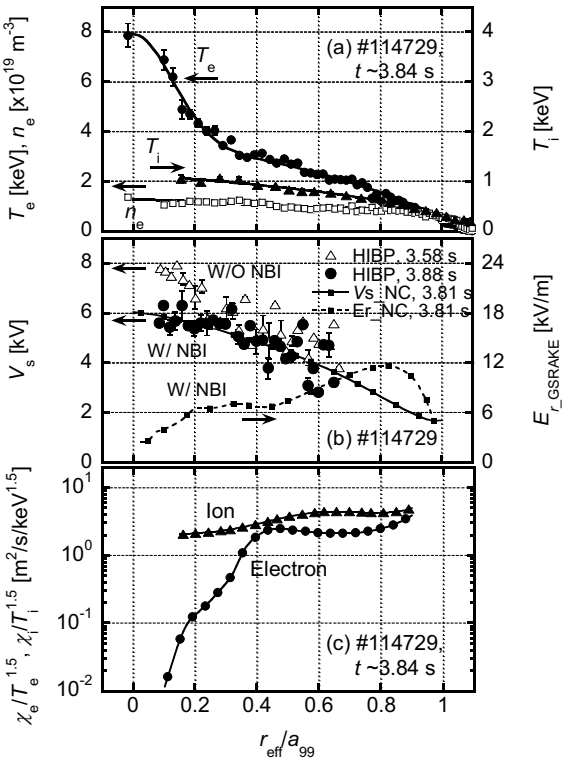

Figure 2. The radial profiles of (a) T_i, T_e and n_e, (b) V_s and E_r and (c) $\chi_e/T_e^{3/2}$ and $\chi_i/T_i^{3/2}$ in the high-T_e plasma.